Hindawi Publishing Corporation
Journal of Nanomaterials
Volume 2012, Article ID 387694, 7 pages
doi:10.1155/2012/387694

Research Article

Synthesis of Bulk Nanostructured DO_{22} Superlattice of $Ni_3(Mo, Nb)$ with High Strength, High Ductility, and High Thermal Stability

H. M. Tawancy

Center for Engineering Research, Research Institute, King Fahd University of Petroleum and Minerals, P.O. Box 1639, Dhahran 31261, Saudi Arabia

Correspondence should be addressed to H. M. Tawancy, tawancyhm@yahoo.com

Received 8 May 2012; Accepted 2 June 2012

Academic Editor: Amir Kajbafvala

We show that a bulk nanostructured material combining high strength, high ductility, and high thermal stability can be synthesized in a Ni-Mo-Nb alloy with composition approaching $Ni_3(Mo,Nb)$. By means of a simple aging treatment at 700°C, the grains of the parent face-centered cubic phase are made to transform into nanosized ordered crystals with DO_{22} superlattice maintaining a size of 10–20 nm after up to 100 hours of aging and corresponding room-temperature yield strength of 820 MPa and tensile ductility of 35%. Deformation of the superlattice is found to predominantly occur by twinning on {111} planes of the parent phase. It is concluded that, although the respective slip systems are suppressed, most of the twinning systems are preserved in the DO_{22} superlattice enhancing the ductility.

1. Introduction

A common feature of bulk nanostructured materials [1–9] and intermetallic compounds [10] is relatively low ductility, which limits their usefulness as engineering materials. In the case of nanostructured materials, deformation behavior is more controlled by grain boundary migration and twinning as opposed to dislocation motion and multiplication. To improve ductility by promoting those deformation modes, research efforts have been focusing on synthesis techniques particularly severe plastic deformation [11–17]. Likewise, there has been an increasing interest in improving the ductility of intermetallic compounds and ordered alloys because of their unique combination of physical and chemical properties [18, 19].

Recently, it has been demonstrated that long-range ordering in Ni-Mo-based alloy can be used to synthesize bulk nanostructured superlattices combining high strength and high ductility [20–24]. It has been shown that the closely-related Pt_2Mo-type (Ni_2Mo), DO_{22} (Ni_3Mo), and $D1_a$ (Ni_4Mo) superlattices coexist during long-range ordering in these systems [22, 23], which form the basis for many commercial alloys with important applications in the chemical process, petrochemical and power generation industries [25]. Each of these superlattices can directly be derived from the parent face-centered cubic structure by minor atoms rearrangement on $\{420\}_{fcc}$ planes. In the case of the Pt_2Mo-type superlattice, every third plane is occupied by Mo atoms and planes in-between contain only Ni atoms. Likewise, for the DO_{22} superlattice, every fourth plane is occupied by Mo atoms, and every fifth plane is occupied by Mo atoms in the case of the $D1_a$ superlattice. Long-range ordering in these systems results in considerable strengthening corresponding to room-temperature yield strength of 800 MPa or higher [22]. However, the corresponding tensile ductility ranges from less than 5% to about 40% depending upon the exact chemical composition, which determines the most stable ordered phase and its morphology. Therefore, by balancing the chemical composition it is possible to synthesize bulk nanostructured superlattices with high strength and high ductility as demonstrated in the case of the $D1_a$ superlattice of Ni_4Mo alloy [21, 22] and Ni-Mo-Cr alloys where the metastable Ni_2Mo with Pt_2Mo-type superlattice is stabilized by controlled amounts of Cr [23, 24]. In the case of binary

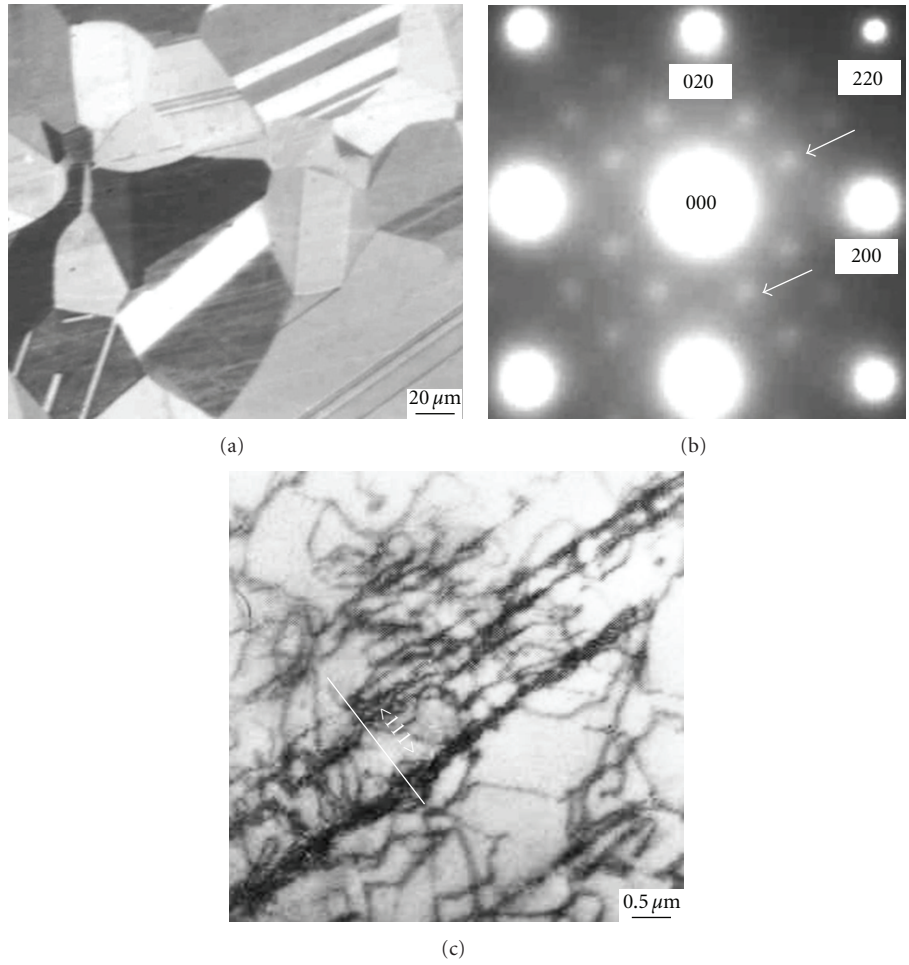

Figure 1: Characteristic structural features of the Ni-Mo-Nb alloy in the annealed condition (15 minutes at 1065°C). (a) Light optical micrograph showing the gross grain structure. (b) <100> selected-area electron diffraction pattern showing {1 1/2 0} short-range order reflections as indicated by the arrows. (c) Bright-field TEM image showing typical deformation substructure corresponding to 10% tensile elongation at room temperature.

Ni_3Mo alloy, large thin platelets of Ni_3Mo form during the earlier stages of thermal aging rendering the material extremely hard and brittle [26]. The objective of this paper is to show that bulk nanostructured DO_{22}-type superlattice with high strength, high ductility, and high thermal stability can be synthesized in a Ni-Mo-Nb alloy with a composition approaching Ni_3(Mo, Nb).

2. Experimental Procedure

The alloy studied had a composition of 64.95 Ni-27.12 Mo-7.93 Nb in weight % corresponding to about 75.2 Ni-18.7 Mo-6.1 Nb in atomic %, approaching the Ni_3(Mo, Nb) composition. Sheets of the alloy about 1.5 mm in thickness were processed by standard techniques of vacuum induction melting, electroslag remelting, forging, hot rolling, and cold rolling. Metallographic specimens (25.4 mm × 25.4 mm × 1.5 mm) and tensile test specimens with 50.8 mm gage length were given recrystallization anneal at 1065°C for 15 minutes followed by water quenching. Specimens for light optical metallography were etched in a solution consisting of 80% HCl and 20% of 15 mol % chromic acid to reveal the initial grain structure. Thermal aging experiments were carried out at 700°C for up to 100 hours followed by air cooling. All tensile tests were conducted at room temperature and the fracture surfaces were examined in the secondary electron mode of a scanning electron microscope operating at 20 keV. Thin foils for transmission electron microscopy were prepared by the jet polishing technique in a solution of 30% nitric acid in methanol. All the foils were examined at an accelerating voltage of 200 keV. Since the parent fcc structure and DO_{22} superlattice are closely related, all diffraction patterns are indexed in terms of the fcc structure.

3. Results and Discussion

Figure 1 summarizes characteristic structural features of the alloy studied in the annealed condition. The gross grain structure is shown in the light optical micrograph of

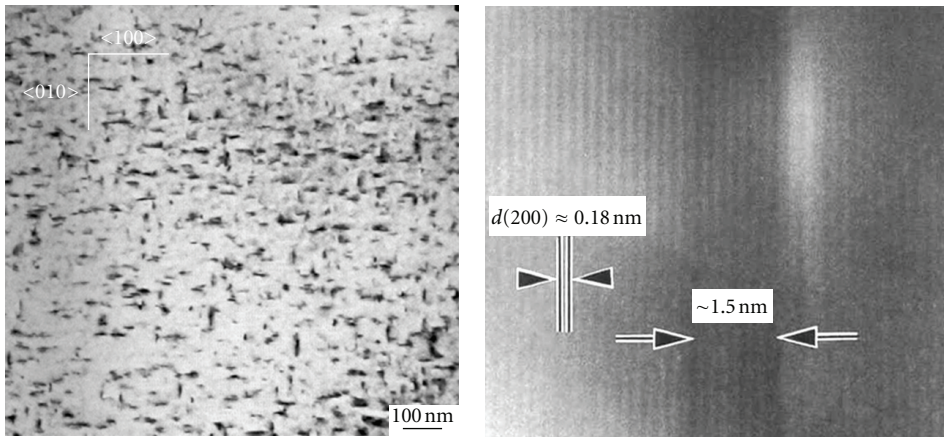

Figure 2: Typical microstructural features observed during the early stages of aging (15 minutes at 700°C). (a) Bright-field TEM image showing nanosized precipitates viewed along <100> direction. (b) Corresponding one-dimensional lattice image of {200} planes showing a highly coherent precipitate with a thickness of about 1.5 nm.

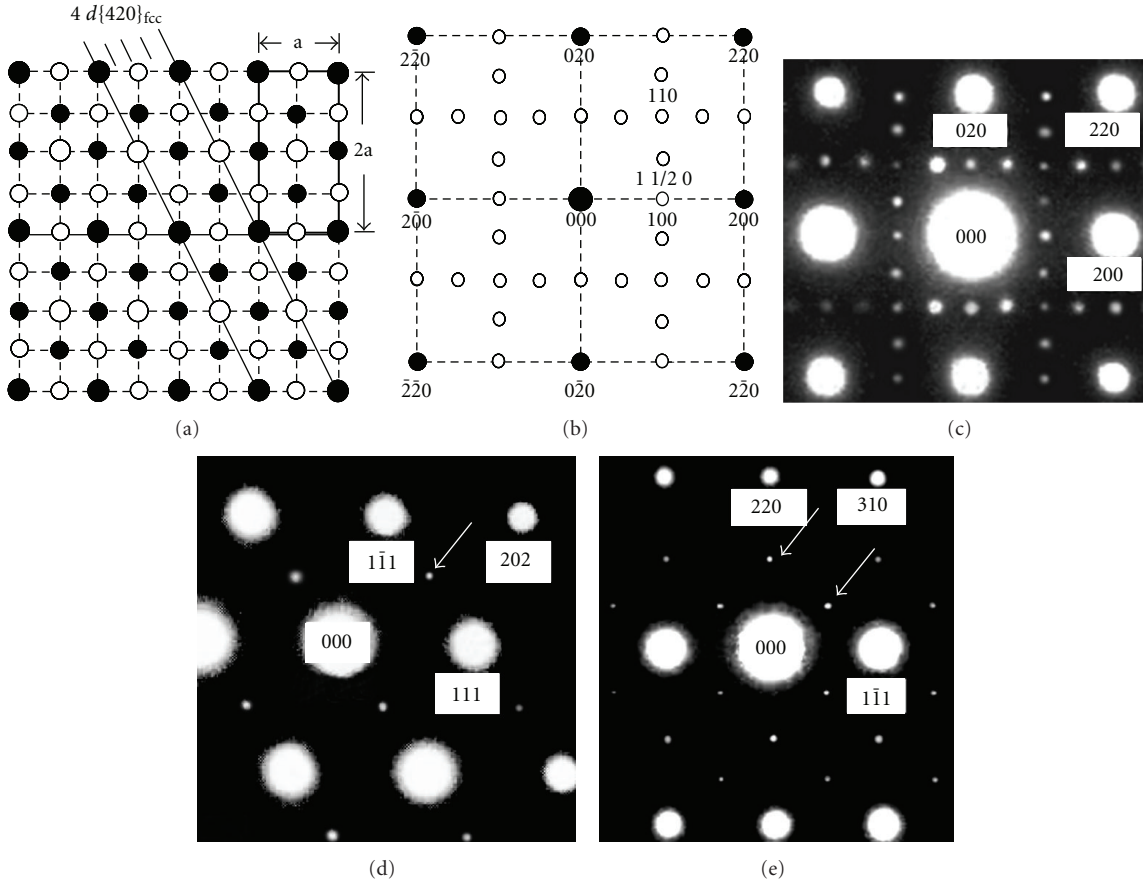

Figure 3: Crystallographic features of the DO_{22} superlattice. (a) Atoms arrangement viewed along <100> direction of the parent fcc lattice showing the tetragonal unit cell of the DO_{22} superlattice: large circles are Mo/Nb atoms (closed circles are atoms at level 0, 1 and open circles are atoms at level 1/2). (b) A schematic of the corresponding <100> reciprocal lattice intersection showing the characteristic DO_{22} superlattice reflections at {1 1/2 0}, {100}, and {110} positions as indicated by the arrows. (c), (d), and (e) are selected-area diffraction patterns derived from specimens aged 24 hours at 700°C in <100>, <110>, and <112> orientations, respectively; the superlattice reflections are indicated by the arrows.

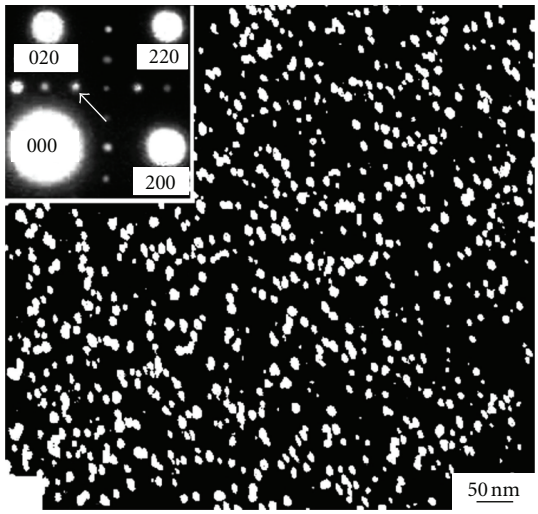

(a)

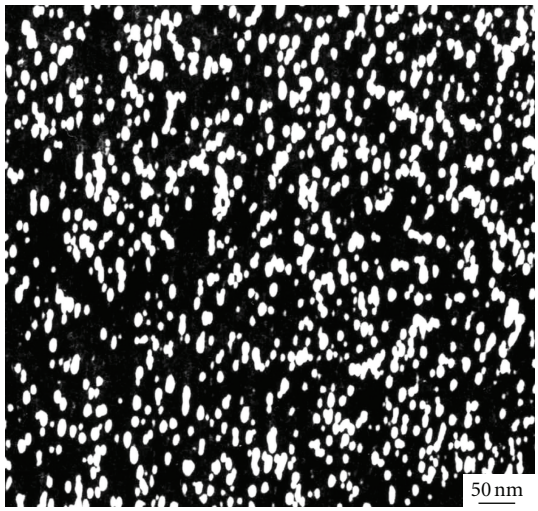

(b)

Figure 4: Dark-field TEM images showing effect of aging time at 700°C on the morphology of one variant of the DO_{22} superlattice. (a) 24 hours of aging; the inset is a section of corresponding <100> diffraction pattern showing the superlattice reflection used to form the image as indicated by the arrow. (b) 100 hours of aging.

Figure 1(a). Full recrystallization is indicated by the high density of annealing twins, which typifies an fcc material with relatively low stacking fault energy [27]. Similar to the case of binary Ni-Mo alloys, the alloy contained short-range order as indicated by the appearance of diffuse intensity maxima at {1 1/2 0} positions in the <100> electron diffraction pattern of Figure 1(b). It has been reported in an earlier study that short-range order tends to lower the stacking fault energy [28]. This is found to be consistent with the observed deformation substructure. As an example, Figure 1(c) is a bright-field TEM image showing the deformation substructure corresponding to 10% tensile elongation at room temperature. Visible slip lines (traces of {111} planes) and the relatively low tendency for

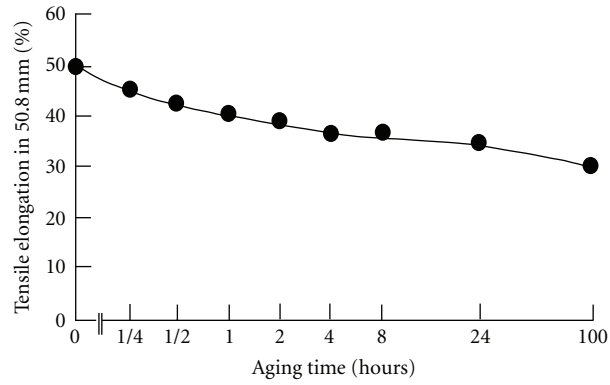

(a)

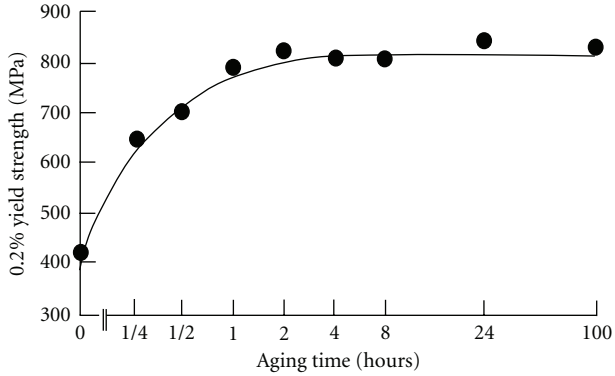

(b)

Figure 5: Effect of aging time up to 100 hours at 700°C on the room-temperature tensile properties. (a) Tensile elongation in 50.8 mm gage length. (b) 0.2% yield strength.

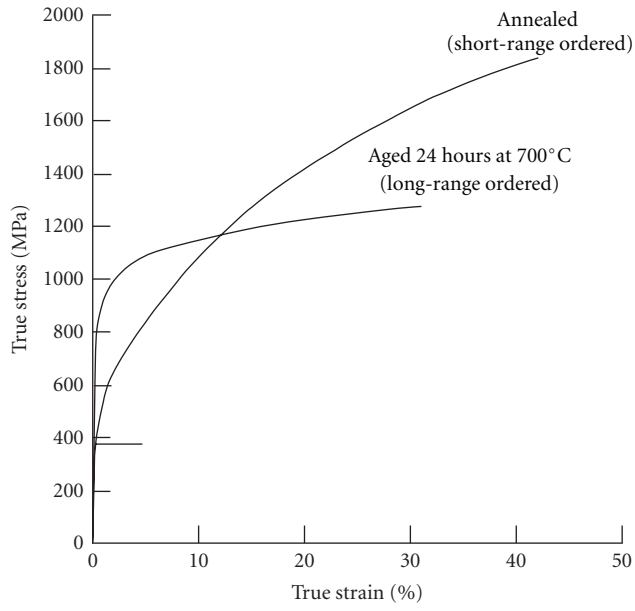

Figure 6: Effect of long-range ordering to the DO_{22} superlattice on the shape of true tensile stress-strain diagram derived at room temperature.

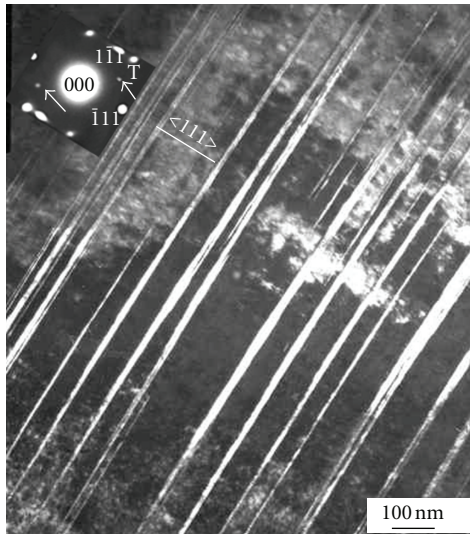

Figure 7: Dark-field TEM image showing {111} twins in the deformation substructure of the DO_{22} superlattice corresponding to 10% tensile elongation at room temperature (the specimen was aged 24 hours at 700°C prior to testing). The inset is the corresponding <110> diffraction pattern showing the twin reflection (T) used to form the image.

dislocation to cross slip are common features of fcc materials having relatively low stacking fault energy [27]. This has an important implication on the preferred deformation mode in the ordered state, which enhances ductility as shown later.

During the early stages of thermal aging (15 minutes at 700°C) very fine precipitates were observed as shown in the example of Figure 2. The bright-field TEM image of Figure 2(a) shows that the precipitates assume the morphology of thin short platelets revealed by elastic strain contrast. At this stage, the precipitates appeared to be too fine to produce characteristic diffraction effects. Figure 2(b) is a one-dimensional lattice image of {200} planes showing a highly coherent precipitate with a thickness of about 1.5 nm. However, with continued thermal exposure, characteristic reflections of the DO_{22} superlattice at {100}, {1 1/2 0}, and {110} positions were observed as demonstrated in Figure 3. A schematic illustration of the crystallographic relationship between the parent fcc lattice and DO_{22} superlattice is given in Figure 3(a). The corresponding {100} reciprocal lattice intersection is shown in Figure 3(b), which is to be compared with the observed <100> diffraction pattern of Figure 3(c) obtained after 24 hours of aging at 700°C. As can be seen, the observed diffraction pattern contains the characteristic reflections of the DO_{22} superlattice. Figures 3(d) and 3(e) show corresponding diffraction patterns in <110> and <112> orientations, respectively, where only {110} reflections can be present in the <110> pattern, and the <112> pattern can contain both the {1 1/2 0}, and {110} superlattice reflections.

Figure 4 shows dark-field TEM images illustrating the ordered microstructure of one crystallographic variant of the DO_{22} superlattice. Both images were formed with

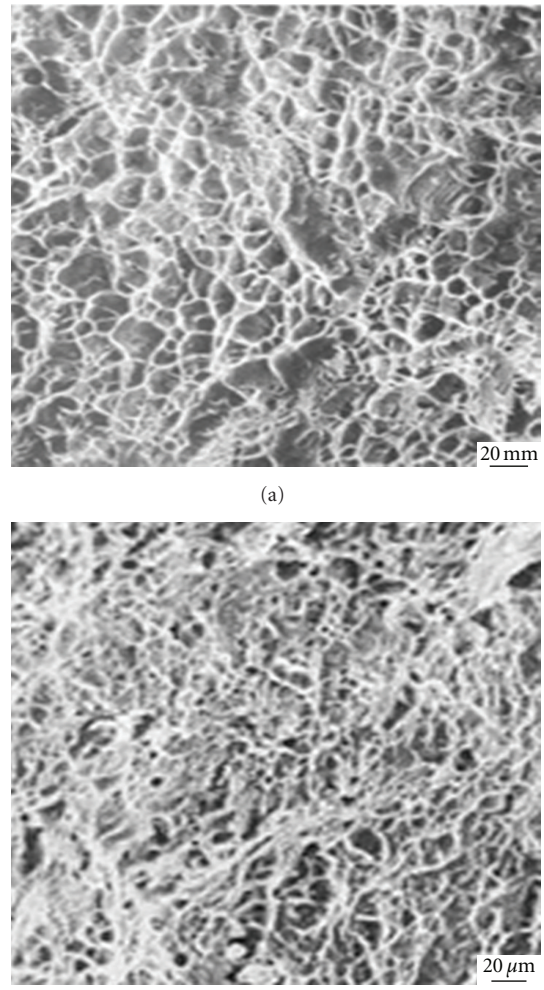

Figure 8: Secondary electron SEM images illustrating comparative tensile fracture surfaces. (a) Annealed (short-range ordered). (b) Aged 24 hours at 700°C (long-range ordered).

{1 1/2 0} superlattice reflections as illustrated in the inset of Figure 4(a). It is observed that the superlattice assumes the morphology of nanosized particles with an average size of 10–20 nm. Also, it is observed as the aging time was extended from 24 hours (Figure 4(a)) to 100 hours (Figure 4(b)), the change in superlattice morphology was insignificant demonstrating its relatively high thermal stability. The corresponding effect of short-range order → long-range order transformation on the room temperature tensile properties is summarized in Figure 5. After 1 hour of aging at 700°C, the 0.2% yield strength was nearly doubled reaching about 800 MPa. However, the material retained about 80% of its initial ductility in the short-range ordered state. With continued aging up to 100 hours, the material maintained a combination of high yield strength of about 820 MPa and high tensile ductility of about 35% consistent with the observed high thermal stability of the DO_{22} superlattice.

Comparative true tensile stress-strain diagrams in the short-range and long-range ordered states are shown in

Figure 6. It is noted that the strain hardening rate is significantly lowered by long-range ordering to the DO_{22} superlattice reflecting a change in the deformation behavior. In contrast with the short-range ordered state where deformation behavior typifies an fcc material with relatively low stacking fault energy as demonstrated in Figure 1(c), twinning on {111} planes is found to be the predominant deformation mode in the long-range ordered state as illustrated in the example of Figure 7. This indicates that although long-range ordering could suppress most of the slip systems characteristic of the parent fcc lattice, many of the twinning systems remain active suggesting that the stacking fault energy of the material is further lowered by long-range ordering enhancing deformation by twinning. A similar behavior is found to occur in ordered Ni-Mo [21, 22] and Ni-Mo-Cr [23, 24] alloys.

Figure 8 shows secondary electron SEM images illustrating the morphology of tensile fractures surfaces in the annealed (short-range ordered) and aged (long-range ordered) states. Typical of ductile materials, in both cases, fracture occurred by dimple-type rupture. However, in the long-range ordered state, the dimples can be seen to be finer and shallower, which could be related to higher density of crack nucleation sites as well as relatively lower ductility in the long-range ordered state.

4. Conclusion

It is concluded that a bulk nanostructured DO_{22} superlattice with high strength, high ductility, and high thermal stability can be synthesized in a Ni-Mo-Nb alloy with composition approaching Ni_3(Mo, Nb) by a simple aging heat treatment at 700°C. Upon thermal aging, the grains of the high-temperature fcc phase are subdivided into ordered crystals on the nanoscale (10–20 nm) with room-temperature yield strength of about 820 MPa and tensile ductility of 35%. Plastic deformation in the ordered state is found to predominantly occur by twinning on {111} planes of the parent fcc structure indicating that the superlattice preserves the twinning systems of the parent phase leading to the observed high ductility.

Acknowledgment

It is a pleasure to acknowledge the continued support of King Fahd University of Petroleum and Minerals.

References

[1] Y. Zhao and X. Liao, "Ductility of bulk nanostructured materials," in *Materials Science Forum*, vol. 633-634, Trans Technical, Zurich, Switzerland, 2010.

[2] C. C. Koch, "Nanostructured materials: an overview," in *Bulk Nanostructured Materials*, M. J. Zehetbauer and Y. T. Zhu, Eds., pp. 1–20, Wiley-VCH, Weinheim Germany, 2009.

[3] E. Bitzek, C. Brandl, P. M. Derlet, and H. Van Swygenhoven, "Dislocation cross-slip in nanocrystalline fcc metals," *Physical Review Letters*, vol. 100, no. 23, Article ID 235501, 4 pages, 2008.

[4] H. Van Swygenhoven and J. R. Weertman, "Deformation in nanocrystalline metals," *Materials Today*, vol. 9, no. 5, pp. 24–31, 2006.

[5] Y. T. Zhu and X. Liao, "Nanostructured metals: retaining ductility," *Nature Materials*, vol. 3, no. 6, pp. 351–352, 2004.

[6] Z. Budrovic, H. Van Swygenhoven, P. M. Derlet, S. Van Petegem, and B. Schmitt, "Plastic deformation with reversible peak broadening in nanocrystalline nickel," *Science*, vol. 304, no. 5668, pp. 273–276, 2004.

[7] C. C. Koch, "Optimization of strength and ductility in nanocrystalline and ultrafine grained metals," *Scripta Materialia*, vol. 49, no. 7, pp. 657–662, 2003.

[8] H. Van Swygenhoven and J. R. Weertman, "Preface to the viewpoint set on: mechanical properties of fully dense nanocrystalline metals," *Scripta Materialia*, vol. 49, no. 7, pp. 625–627, 2003.

[9] D. Jia, Y. M. Wang, K. T. Ramesh, E. Ma, Y. T. Zhu, and R. Z. Valiev, "Deformation behavior and plastic instabilities of ultrafine-grained titanium," *Applied Physics Letters*, vol. 79, no. 5, pp. 611–613, 2001.

[10] R. W. Cahn, "Intermetallics: new physics," *Contemporary Physics*, vol. 42, no. 6, pp. 365–375, 2001.

[11] P. Xue, B. L. Xiao, and Z. Y. Ma, "High tensile ductility via enhanced strain hardening in ultrafine-grained Cu," *Materials Science and Engineering A*, vol. 532, pp. 106–110, 2012.

[12] D. G. Morris and M. A. Munoz-Morris, "Microstructural refinement in alloys and intermetallics by severe plastic deformation," *Journal of Alloys and Compounds*. In press.

[13] K. V. León, M. A. Muñoz-Morris, and D. G. Morris, "Optimisation of strength and ductility of Cu-Cr-Zr by combining severe plastic deformation and precipitation," *Materials Science and Engineering A*, vol. 536, pp. 181–189, 2012.

[14] Y. Zhao, Y. Zhu, and E. J. Lavernia, "Strategies for improving tensile ductility of bulk nanostructured materials," *Advanced Engineering Materials*, vol. 12, no. 8, pp. 769–778, 2010.

[15] M. A. Muñoz-Morris and D. G. Morris, "Severe plastic deformation processing of Al-Cu-Li alloy for enhancing strength while maintaining ductility," *Scripta Materialia*, vol. 63, no. 3, pp. 304–307, 2010.

[16] Y. Zhao, T. Topping, J. F. Bingert et al., "High tensile ductility and strength in bulk nanostructured nickel," *Advanced Materials*, vol. 20, no. 16, pp. 3028–3033, 2008.

[17] R. Z. Valiev, "The new trends in fabrication of bulk nanostructured materials by SPD processing," *Journal of Materials Science*, vol. 42, no. 5, pp. 1483–1490, 2007.

[18] K. A. Gschneidner, M. Ji, C. Z. Wang et al., "Influence of the electronic structure on the ductile behavior of B2 CsCl-type AB intermetallics," *Acta Materialia*, vol. 57, no. 19, pp. 5876–5881, 2009.

[19] K. Gschneidner, A. Russell, A. Pecharsky et al., "A family of ductile intermetallic compounds," *Nature Materials*, vol. 2, no. 9, pp. 587–590, 2003.

[20] H. M. Tawancy, "Corrosion resistant Nickel-Base Alloys," US Patent no. 7, 922, 969, 2011.

[21] H. M. Tawancy and M. O. Aboelfotoh, "Yttrium-doped nanocrystalline Ni_4Mo: ultrahigh strength and high ductility combined with useful intermetallic properties," *Journal of Materials Science*, vol. 45, no. 13, pp. 3413–3418, 2010.

[22] H. M. Tawancy, "Long-range ordering: an approach to synthesize nanoscale Ni-Mo-based superlattices with high strength and high ductility," *Materials Science Forum*, vol. 633-634, pp. 421–435, 2010.

[23] H. M. Tawancy and M. O. Aboelfotoh, "Application of long-range ordering in the synthesis of a nanoscale Ni_2 (Cr,Mo)

superlattice with high strength and high ductility," *Materials Science and Engineering A*, vol. 500, no. 1-2, pp. 188–195, 2009.

[24] H. M. Tawancy and M. O. Aboelfotoh, "High strength and high ductility in a nanoscale superlattice of Ni_2(Cr,Mo) deformable by twinning," *Scripta Materialia*, vol. 59, no. 8, pp. 846–849, 2008.

[25] F. G. Hodge, "Nickel and high-nickel alloys," in *Corrosion and Corrosion Protection Handbook*, P. A. Schweitzer, Ed., pp. 65–69, Marcel-Dekker, New York, NY, USA, 1983.

[26] H. M. Tawancy, "Long-range ordering behaviour and mechanical properties of Ni-Mo-based alloys," *Journal of Materials Science*, vol. 30, no. 2, pp. 522–537, 1995.

[27] P. R. Swann, "Dislocation arrangements in face-centered cubic materials," in *Electron Microscopy and Strength and Crystals*, G. Thomas and J. Washburn, Eds., pp. 131–181, Wiley Interscience, New York, NY, USA, 1963.

[28] P. R. Okamoto and G. Thomas, "On short range order and micro-domains in the Ni_4Mo system," *Acta Metallurgica*, vol. 19, no. 8, pp. 825–841, 1971.